ADVANCES IN COMPUTATIONAL AEROACOUSTICS: CHALLENGES AND ISSUES

C. Bailly[1,2], *C. Bogey*[1] *and O. Marsden*[1]

[1] *Laboratoire de Mécanique des Fluides et d'Acoustique*
UMR CNRS 5509 & Ecole Centrale de Lyon
[2] *Institut Universitaire de France*

christophe.bailly@ec-lyon.fr

Abstract

Needs of accurate and efficient numerical solvers in computational aeroacoustics have motivated the development of low-dispersion and low-dissipation schemes as an alternative to more classical methods of applied mathematics for computational fluid mechanics over the last two decades. These numerical methods have now reached maturity, even if progress is still necessary to take account of specific physics. The paper provides a short overview of some recent developments and applications involving these topics, and is organized as follows. Motivations and numerical advances are considered, but the main part of this synthesis focuses on the use of these simulations to improve our understanding of noise generation by turbulent flows. Applications to subsonic and supersonic jet noise, cavity noise and self-excited internal flows are thus presented.

1 Motivations

The spectacular development of computational aeroacoustics since the beginning of the nineties has allowed the emergence of the direct computation of aerodynamic noise, which is now technically mature. There is still a lot of scope for progress, in particular for the numerics and for the strategies to implement for more complex configurations, but direct noise calculation is currently a reliable and accurate tool, which reproduces studied physics with high fidelity. Direct Noise Computation (DNC) consists in solving compressible Navier-Stokes equations to determine simultaneously the aerodynamic field and the acoustic field in a same domain. This approach is quite different from more classical modellings for which aerodynamics and acoustics are decoupled, such as Lighthill's analogy. It is consequently rather natural to apply this approach for studying in more detail noise mechanisms and modelling, and for evaluating noise reduction solutions. The resolution of more theoretical problems concerning aeroacoustics and propagation in the presence of a flow can also be performed by this way.

Note that recent excellent technical reviews on computational aeroacoustics are available by Colonius and Lele (2004), Wang, Freund & Lele (2006) or by Colonius (2004) for the key problem of non-reflecting boundary conditions. Therefore, the present contribution does not restate the topics already tackled.

The organization of this paper is as follows. The constant progress of numerics is outlined in section 2 by the presentation of an optimized low-storage 4th-order Runge-Kutta scheme for which the dissipation error is spectacularly reduced. Section 3 is devoted to noise radiated by round subsonic jets, and thus to broadband noise associated with high-Reynolds-number turbulent free shear flows. Analysis of noise sources by a causality method is illustrated. In sections 4 and 5, noise radiated by a planar imperfectly expanded supersonic jet and by self-induced supersonic flow oscillations behind a sudden enlargement are discussed. In these two examples, the presence of a feedback mechanism and/or of resonances for internal flows often introduces a frequency selection. The involved scales, *e.g.* scales associated with wall flows, shocks and acoustic resonances in duct flows, are also strongly disparate. In section 6, the simulation of an adaptive control to reduce cavity noise is presented. Concluding remarks and works in progress are finally provided.

2 Numerics

The algorithms used in the direct noise computation require a continuous effort of development to improve numerical efficiency, allowing to deal with more complex configurations including physics and geometry. A review of the use of finite-difference schemes is available in Bailly and Bogey (2006). As an example of recent development which could significantly improve numerical simulations, the optimized Runge-Kutta scheme developed by Berland *et al.* (2006) is now discussed. This point illustrates the effort in applied mathematics to make progress in the development of low-dispersion and low-dissipation schemes for solving unsteady problems in fluid mechanics.

Consider the following semi-discrete differential

equation

$$\frac{\partial u^n}{\partial t} = F(u^n, t)$$

where $u^n(x) = u(x, n\Delta t)$. From the time Fourier transform defined as

$$u(t) = \int_{-\infty}^{+\infty} \hat{u}(\omega) e^{-i\omega t} d\omega$$

an amplification factor $R_s = \hat{u}^{n+1}/\hat{u}^n$ can be calculated. The integration error is estimated by comparison between the exact amplification factor given by $R_e = e^{-i\omega\Delta t}$ and the effective amplification factor of the scheme, which takes the following form

$$R_s = 1 + \sum_{j=1}^{p} \gamma_j (-i\omega\Delta t)^j \qquad (1)$$

Stability requires an amplification rate so that $|R_s(\omega\Delta t)| < 1$, and integration errors can be measured by comparing $R_s = |R_s| e^{-i\omega_s \Delta t}$ with the exact amplification factor R_e, in terms of dissipation error with $1-|R_s|$, and of phase error with $|\omega_s\Delta t - \omega\Delta t|/\pi$.

The amplification rates of some classical schemes are reported in Fig. 1 as a function of the normalized angular frequency $\omega\Delta t$. For frequency up to four points per wavelength, *i.e.* $\omega\Delta t \leq \pi/2$, there is more than three orders of magnitude between the dissipation of the classical Runge-Kutta scheme and the optimized low-storage scheme of Berland *et al.* (2006), both providing a formal 4th-order integration. Note also the good behaviour of the optimized scheme for the phase error, and the large time-step range of stability, $\omega\Delta t < 3.82$, with respect to the classical Runge-Kutta scheme yielding $\omega\Delta t < 2\sqrt{2} \simeq 2.83$.

Again this example is reported to emphasize that new efficient algorithms have been developed over the last years, with the aim of controlling numerical dispersion and dissipation for solving unsteady nonlinear problems.

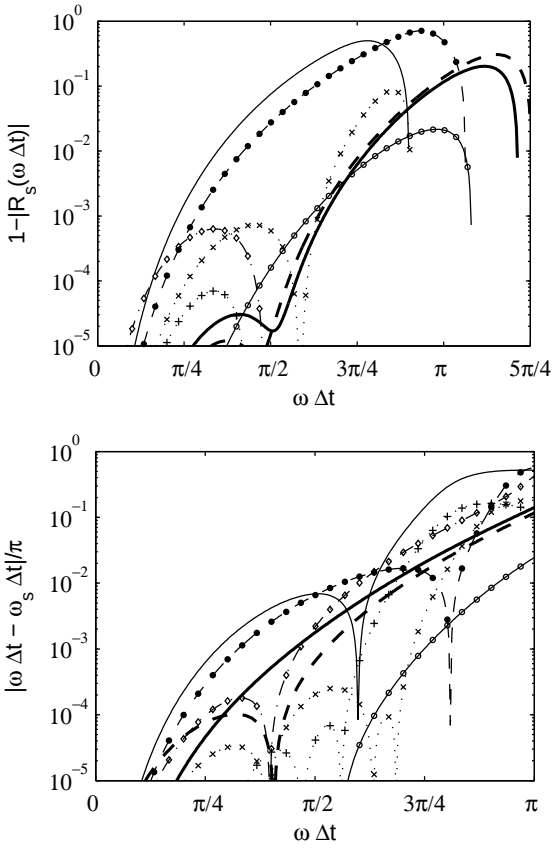

Figure 1: Modulus and phase error of the amplification factor (1) as a function of the angular frequency, plotted in logarithmic scale. —— standard 4th-order RK, $-\circ-$ standard 8th-order RK, $\cdots+\cdots$ LDDRK46 Hu (1996), $\cdots\times\cdots$ LDDRK56 Hu (1996), $-\bullet-$ 4th-order 2N-RK Carpenter (1994), $-\cdot\diamond-\cdot$ opt. 4th-order 2N Stanescu (1998), **- - -** opt. 2nd-order RK Bogey (2004), **——** opt. 4th-order 2N-RK Berland (2006).

3 Subsonic jet noise

The prediction of subsonic jet noise is one of the oldest topics of aeroacoustics even if our understanding of noise mechanisms remains incomplete. The final goal of all these research works is the reduction of noise in urban environments. Indeed society cannot tolerate additional noise pollution, and traffic growth must be compensated by innovative noise reduction methods. This environmental challenge is also strategic for the economic development of the aeronautics industry.

As pointed out in the introduction, the direct computation of aerodynamic noise using compressible large-eddy simulations is approaching maturity, and subsonic jet noise has been one of the first applications, with the direct numerical simulation of Freund (2001) of a jet at Mach number 0.9 and at Reynolds number 3600, which is based on the jet exit velocity and the jet diameter. The grid requirement of direct numerical simulations is however difficult to satisfy for the computations of laboratory experiments with typical Reynolds number Re_D of about $10^5 - 10^6$. Moreover, overall flow and noise characteristics are no longer dependent on the Reynolds number for roughly $\mathrm{Re}_D \geq 2.5\times10^5$. This observation is directly linked to the laminar or turbulent state of the nozzle exit boundary layer. Therefore, compressible large-eddy simulations appear to be relevant to develop direct noise computation and to reproduce Reynolds effects.

To illustrate this point, Fig. 2 displays snapshots of the vorticity norm and of the fluctuating pressure for jets at Mach number 0.9 but at different Reynolds numbers in order to investigate alterations on the flow development and on the radiated acoustic field. In the present work, the LES strategy is based on explicit selective filtering with spectral-like resolution combined with low dispersion and low dissipation numerical algorithms, see Bogey and Bailly (2006b) for a discussion. As the Reynolds number decreases, the jet

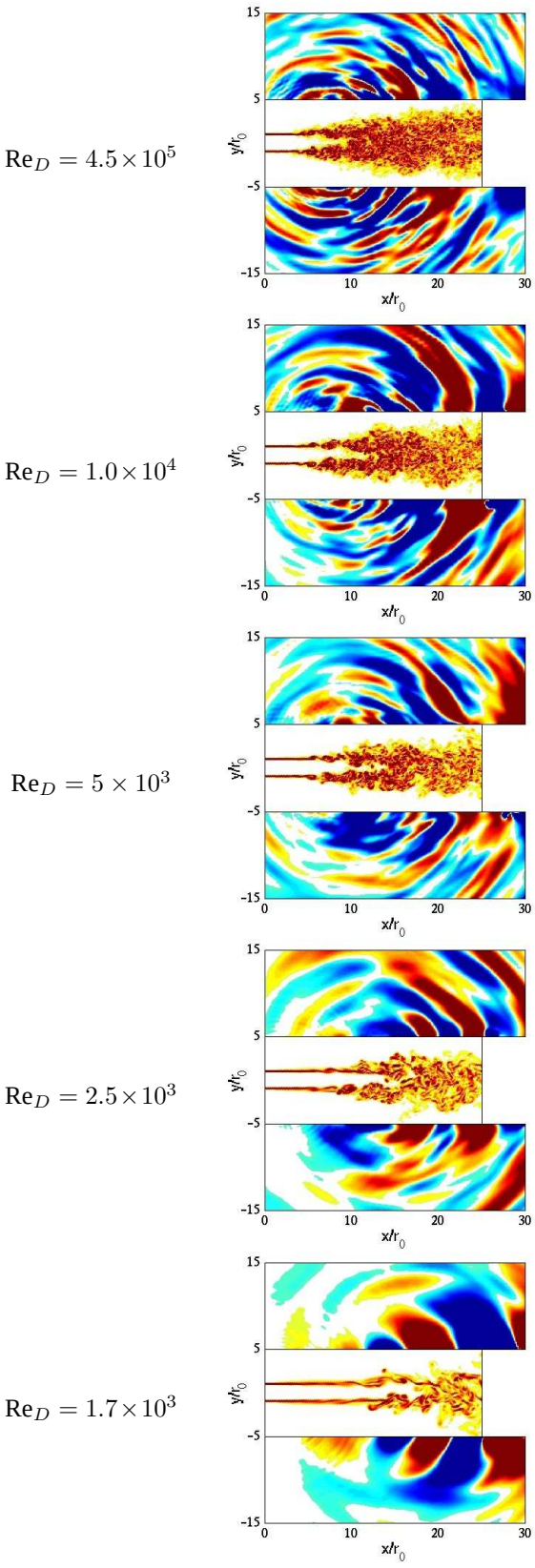

Figure 2: Jets at Mach M $= 0.9$. Snapshots of the vorticity norm $|\boldsymbol{\omega}|$ in the flow and of the fluctuating pressure p' outside, in the plane $z = 0$. For the five simulations, the color scale of the vorticity norm is $|\boldsymbol{\omega}| \times r_0/u_j = [0, 2.65]$, and the pressure color scale is $p' = [-70, 70]$ Pa or $p'/(\rho_j u_j^2) = [-6.2, 6.2] \times 10^{-4}$.

flow changes significantly, and develops more slowly upstream of the end of the potential core, but more rapidly downstream. The acoustic field radiated in the sideline direction appears to vanish progressively as the Reynolds number is decreased, which can be directly linked to the absence of fine scale turbulence in the shear layers. Quantities such as mean velocity, jet spreading, turbulence intensity, integral length scales, spectra, acoustic azimuthal correlations and power laws have also been investigated as a function of the observer angle for circular jets at Mach number 0.6 and 0.9, with Reynolds numbers varying from 1.7×10^3 to 4×10^5 by Bogey and Bailly (2006a, 2006b). The simulations suggest the presence of two sound sources: a Reynolds-number-dependent source, predominant for large radiation angles, connected to the randomly-developing turbulence, and a deterministic source, radiating downstream, related to a mechanism intrinsic to the jet geometry, which is still to be comprehensively described. This view agrees well with the experimental results displaying two distinguishable components in turbulent mixing noise.

Furthermore for the acoustic spectra of the two apparent contributions, frequency scaling by a Strouhal number, St $= fD/u_j$, f being the frequency, D the jet diameter and u_j the jet velocity, appears both suitable . However, the evolution of the peak is clearly different in the two directions, namely in the sideline direction and in the downstream direction. For observation angles $\theta \simeq 90\,\mathrm{deg}$, the spectral peak is Strouhal-dependent, and must be connected to the turbulence development in the shear layers between the nozzle and the end of the potential core. This evolution is also clearly visible on spectra. In the downstream direction, the frequency is weakly dependent on the Reynolds number, with St $\simeq 0.25$, and this radiation can be linked to the periodic intrusion of vorticity at the end of the potential core.

The acoustic radiation by the turbulence developping in the shear layers seems partially understood, and active control or flow forcing by impinging microjets could be applied to achieve noise reduction. On the contrary, the noise mechanism at the end of the potential core is not well explained with our current knowledge of jet noise. Frequency selection of a global mode for subsonic cold jets is not predicted by the instability theory for instance, and is still to be clearly described. Based on this remark, it should be also underlined that there is still a role for theory, in particular to support the interpretation of these simulations.

Another possible way to establish direct links between turbulent flow events and emitted sound waves and to help towards the identification of noise-source mechanisms, is to apply a causality method to LES data, as proposed in Bogey and Bailly (2007). For that, the normalized cross-correlation between the jet turbulence at $(\boldsymbol{x}_1, t_0)$ and the radiated pressure $(\boldsymbol{x}_2, t_0 + t)$

is introduced:

$$C_{fp}\left(\boldsymbol{x}_1,\boldsymbol{x}_2,t\right)=\frac{\left\langle f(\boldsymbol{x}_1,t_0)\,p'(\boldsymbol{x}_2,t_0+t)\right\rangle}{\left\langle f^2(\boldsymbol{x}_1,t_0)\right\rangle^{1/2}\left\langle p'^2(\boldsymbol{x}_2,t_0)\right\rangle^{1/2}}$$

where the quantity f is any relevant calculated variable of the direct noise computation. Results are reported in Fig. 3 where f is the norm of the vorticity along the jet axis. The particular role played by the flow dynamic at the end of the potential core is again emphasized for the noise radiated in the downstream direction whatever the Reynolds number may be. This kind of investigation clearly needs more work using advanced signal processing and alternative localization techniques such as antenna or conditional statistics.

To conclude and to provide a critical review, even if high-fidelity flow and noise simulations are now performed, it remains some difficulties such as the generation of artificial turbulence at the inflow boundary conditions to mimic the turbulent boundary layer or the thicker boundary layers used in numerical simulations, typically $\delta_\theta/D \sim 10^{-2}$ instead of 10^{-3} in experiments, leading to some potential shifts with measurements for the potential core length or spectral peaks in the initial shear-layer.

4 Supersonic jet noise

Additional noise generated by supersonic jets, and especially screech tones, contribute significantly to acoustic fatigue of combat aircrafts. Shock-associated noise radiates primarily in the upstream direction and consequently increases also notably cabin noise of modern commercial aircrafts.

Noise of imperfectly expanded supersonic jets has been studied experimentally and theoretically in order to identify the interactions between turbulence and the quasi-periodic shock-cell structure. These interactions generate upstream-propagating sound waves. A resonant loop is then obtained when acoustic waves are diffracted by the nozzle lips and thus excite the initial shear layers. However, predictions are still qualitative and provide basically the fundamental frequency associated with the feedback loop. Further details can be found in the review paper of Raman (1999). The determination of the amplitude of the radiated acoustic field remains a difficult challenge, and is directly connected to a clear understanding of the shock - vortex interaction, as proposed by Suzuki and Lele (2003) for the case of a planar shear layer.

This issue has been recently investigated by Berland *et al.* (2007) with the compressible large eddy simulation of screech tones generated by a three-dimensional planar underexpanded jet. The jet operates at fully expanded Mach number $\mathrm{M}_j = 1.55$, with a Reynolds number $\mathrm{Re}_h = 6\times10^4$ based on the jet exit velocity u_j and of the nozzle height h. The ratio between the exit pressure and the ambiant pressure is $p_e/p_\infty = 2.09$, corresponding to maximum screech

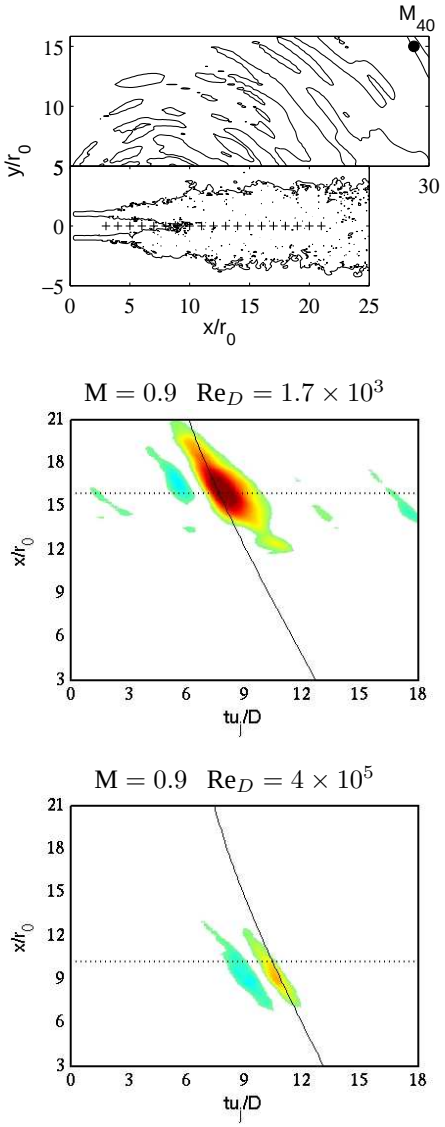

Figure 3: Correlation coefficient $C_{\omega p}(x/r_0, tu_j/D)$ between the vorticity along the jet axis at $+\ \boldsymbol{x}_1 = (x,0,0)$ and the acoustic field at $\bullet\ \boldsymbol{x}_2 = M_{40}$. Time delay tu_j/D versus axial distance x/r_0, —— time of propagation at the speed of sound, ····· end of the potential core $x = x_c$, color scale: [-0.14 0.14] (white: [-0.035 0.035]).

noise generated by a rectangular nozzle with large aspect ratio, as shown experimentally by Krothapalli *et al.* (1986). Numerical parameters and validations can be found in the paper previously mentioned. The flow and especially the shock-cell structure are in agreement with the literature. Furthermore the upstream acoustic field exhibits harmonic tones that compare correctly to screech tones observed on rectangular jets in terms of frequency, amplitude and phase shift on both sides of the jet. As an illustration, Fig. 4 displays a snapshot of the direct noise computation. Compression shocks corresponding to high-density gradients are seen inside the jet plume. Upstream-propagating

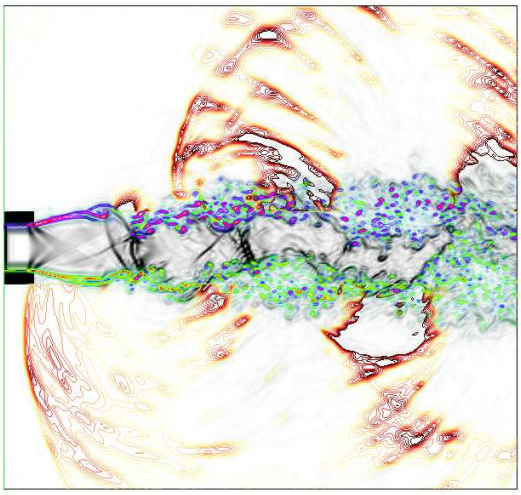

Figure 4: Computation of the generation of screech tones in an underexpanded supersonic jet, fully expanded jet at Mach number 1.55, Reynolds number 6×10^4. Snapshot of the density modulus, of the spanwise vorticity and of the near-field pressure, in a plane perpendicular to the spanwise direction. The nozzle lips are represented in black. From Berland *et al.* (2007).

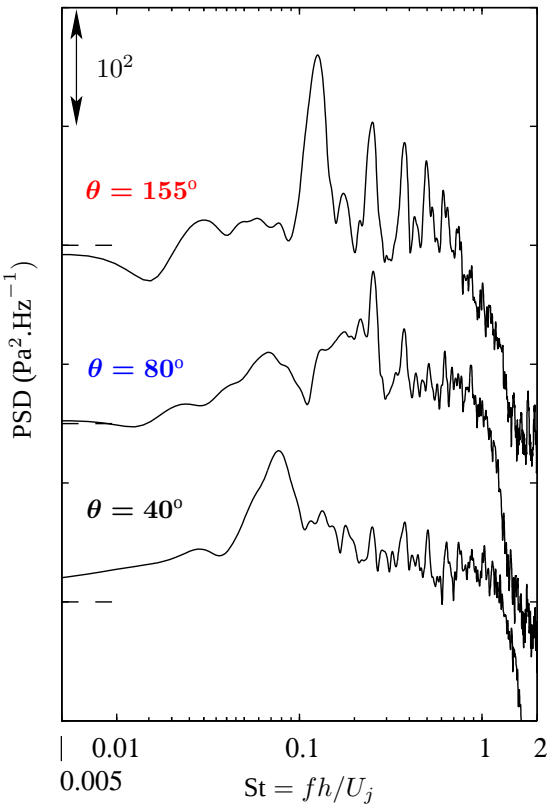

Figure 5: Computation of the generation of screech tones in an underexpanded supersonic jet, fully expanded at jet Mach number 1.55, Reynolds number 6×10^4. From Berland *et al.* (2007).

wave-fronts associated with screech tones radiation are also clearly visible on both sides of the jet. The Strouhal number corresponding to the screech frequency is equal to St $= f_s h/u_j \simeq 0.126$. A further study of the simulation data has permitted to locate the screech source near the third shock-cell, as noticed in the experiments of Krothapalli *et al.* (1986) among others, and to provide evidences of the connection between the shock-leakage process, proposed by Suzuki and Lele (2003), and the generation of screech tones.

The far-field noise is extrapolated by using the linearized Euler equations in order to compute acoustic spectra. Power spectral densities of the pressure fluctuations are reported in Fig. 5 for different observation angles θ with respect to the downstream direction. Three contributions can be found: screech noise, broadband shock-associated noise and mixing noise which has already been discussed in the previous section devoted to subsonic jet noise. For $\theta = 155\,\mathrm{deg}$, the spectrum is dominated by the fundamental screech tone and its harmonics. For an observer in the sideline direction, $\theta = 80\,\mathrm{deg}$, the fundamental screech tone is no longer visible whereas its first harmonic dominates the radiated field. Two broadband peaks can also be noticed, a low-frequency contribution at St $\simeq 0.07$ associated with the mixing noise and a higher frequency contribution around $0.1 \leq$ St ≤ 0.2. In the downstream direction, at $\theta = 40\,\mathrm{deg}$, the mixing noise becomes the principal noise source. As pointed out by Tam *et al.* (1986), a relationship exists between the frequency peak f_p of broadband shock-associated noise

$$\frac{f_p h}{c_\infty} \simeq M_c \, \frac{h}{L_s(1 - M_c \cos\theta)}$$

and those of screech noise $f_s = \lim_{\theta \to \pi} f_p$, where $M_c = u_c/c_\infty \simeq 0.55 u_j/c_\infty$ is the convection Mach number and L_s is the shock cell spacing, approximated by $L_s \simeq 2h(M_j^2 - 1)^{1/2}$ for a two-dimensional jet, see Tam (1988).

The present simulation is thus able to capture the three noise sources and to correctly reproduce broadband spectra as a function of the observer position, in agreement with the literature, as summarized by Tam (1995) or by Raman (1999).

5 Self-excitated oscillations in internal flows

Shock-induced flow oscillations behind a sudden enlargement of cross-section are frequently generated by pressure-reducing valves and by flow control devices in pipe systems of power plants. This configuration is also representative of transonic and supersonic flows involving unstable shock patterns yielding noise production increase, as discussed in the survey paper of Meier *et al.* (1990).

The present studied configuration, displayed in Fig. 6, has been investigated experimentally for dif-

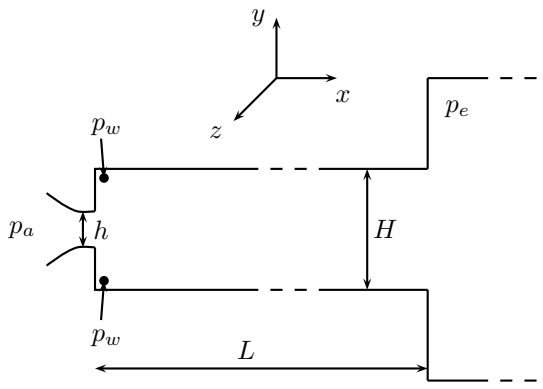

Figure 6: Sudden enlargement of rectangular duct cross-section: the flow regime is characterized by the pressure ratio between the plenum chamber and the reservoir pressure $\tau = p_e/p_a$. The area ratio is given by h/H, where h is the nozzle height and H the height of the test-duct; L is the duct length and b is the width of the nozzle and of the duct. The flow can be monitored by the base pressure p_w at the two upstream corners of the channel.

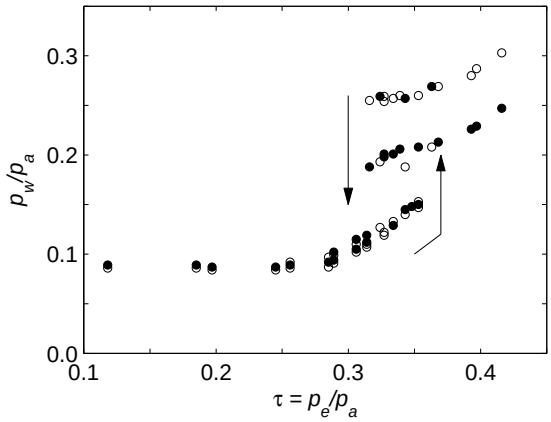

Figure 7: Turbulent flow behind a sudden enlargement of rectangular duct cross-section for the case $L = 0.16$ m, $L/H = 5.23$ and $h/H = 0.3$. Experimental data of the upper ○ and lower • normalized mean base pressure p_w/p_a as a function of the pressure ratio τ, from Anderson *et al.* (1977).

ferent values of the area ratio h/H and of the channel length L/H. Boundary layer - shock wave interactions as well as possible flow oscillations, hysteresis phenomena and coupling with acoustic duct resonance are reported by Anderson *et al.* (1977) and by Meier *et al.* (1978).

The evolution of the mean base pressure p_w/p_a as a function of the pressure ratio τ is shown in Fig. 7 for a given duct geometry. For lower values of the pressure ratio, $\tau \leq 0.25$, the mean base pressure p_w is nearly constant. The symmetrical and steady flow pattern is structured by reflected oblique shock waves interacting with the boundary layers. Increasing the plenum-chamber pressure p_e, and thus the pressure ratio $\tau = p_e/p_a$ where p_a is the reservoir pressure, leads to a decrease and at the end, to a breakdown of the periodic shock-cell structure. For higher pressure ratio, the flow becomes asymmetric and is attached to either the upper or the lower wall of the channel yielding two values of the base pressure p_w. An hysteresis phenomenon is also observed experimentally, indicated by the two arrows in Fig. 7 Moreover a self-excited flow configuration can occur for $0.31 \leq \tau \leq 0.35$, and under particular conditions, a strong coupling is found with longitudinal acoustic modes of the channel, at frequencies given by

$$f = (2n-1)\frac{c}{4L}(1-\bar{M}^2) \qquad n = 1, 2, \ldots$$

where $\bar{M}$ is the averaged Mach number along the channel axis.

This flow has been carefully studied in Emmert *et al.* (2007) by compressible large-eddy simulations based on a high-order algorithm and an additional non-linear adaptive filtering combined with high-order overlapping grid technique. Schlieren pictures of two computed regimes among others, are displayed in Fig. 8. For $\tau = 0.31$, a symmetrical flow pattern is found with a normal shock wave in the channel. A characteristic lambda structure for the shock foot is observed as well as interactions with wall boundary layers producing their thickening behind the shock. In the case $\tau = 0.32$, an asymmetrical separated flow is found with attachement to the upper side of the channel. The switching between the symmetrical and asymmetrical flow patterns as well as the predicted values for the base pressure have been accurately reproduced by the simulations. A case of strong coupling between shock oscillations and a longitudinal acoustic mode is also reported by Emmert *et al.* (2007).

The simulation of such configurations involving turbulence, boundary layers, shocks and coupling through acoustic resonances is currently challenging. The hysteresis cycle described in Fig. 7 and the symmetric or asymmetrical state taken by the shock pattern is strongly dependent on the correct description of the turbulent boundary layers as well as of the impedance conditions at the boundaries of the computational domain. A suitable truncature of the physical domain is also of importance.

6 Simulation of the application of an adaptive control to a cavity flow

Cavity noise, which occurs when a cavity is placed in a grazing flow, is of increasing concern to both military applications for the flow inside the cavity, and to transport industry for the radiated far-field noise. Instabilities are shed by the upstream cavity corner and are simultaneously convected and amplified by the shear layer until they impact the downstream cavity

(a) $\tau = 0.31$

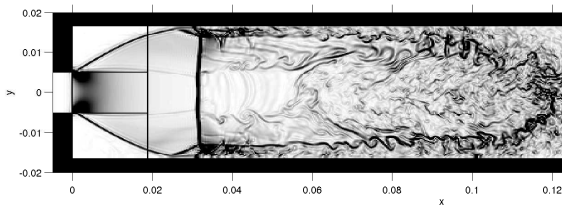

(b) $\tau = 0.32$

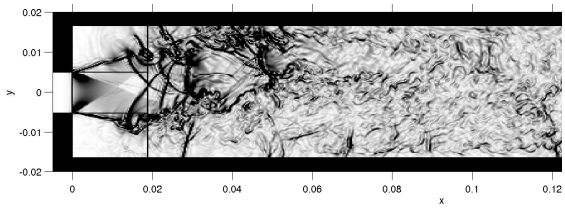

Figure 8: Compressible large-eddy simulation of the turbulent flow behind a sudden enlargement of rectangular duct cross-section: snapshot of density gradient $|\nabla\rho|$ for two pressure ratios for the case $L = 0.16$ m, $L/H = 5.23$ and $h/H = 0.3$. See Emmert *et al.* (2007).

wall, thus generating noise. Pressure waves induced by the impact can create a feedback loop by synchronising the upstream shear layer oscillations, resulting in very high pressure fluctuation levels. Active control techniques have been investigated experimentally as a possible mean of reducing noise generation. Recent syntheses of the extensive litterature can be found in Cattafesta *et al.* (2003) or in Rowley and Williams (2006).

A direct simulation of a closed-loop active control to reduce cavity noise is reported in the present section. A leaky-LMS algorithm has been used and implemented in the compressible Navier-Stokes solver developed by Gloerfelt *et al.* (2003) to show the feasability of the control itself, and of the numerical coupling. The simulated cavity is shown in Fig. 9. The cavity is 2 mm long, with $L/D = 1$ and $L/W = 1.28$. The upstream flow has a Mach number of $M = 0.6$ and a Reynolds number based on the cavity depth of $Re_D = 28720$. The upstream boundary layer is laminar, with $L/\delta_\theta = 57$. A simple form of pulsed injection is used as the control actuator. It consists in adding a control term to momentum equation on ρv where v is the vertical velocity, inside the time integration. This term is introduced on a zone whose envelope is Gaussian in the x and y directions and of half-width $L/50$ in both directions. The injection zone, spanning the entire width of the cavity, is placed immediately after the upstream corner, as shown in Fig. 9. The error signal supplied to the control algorithm is the pressure perturbation $p' = p - p_\infty$ measured slightly underneath the impact zone on the downstream cavity wall and averaged over five sensors in the spanwise direction.

The stability of the controlled cavity is one of the

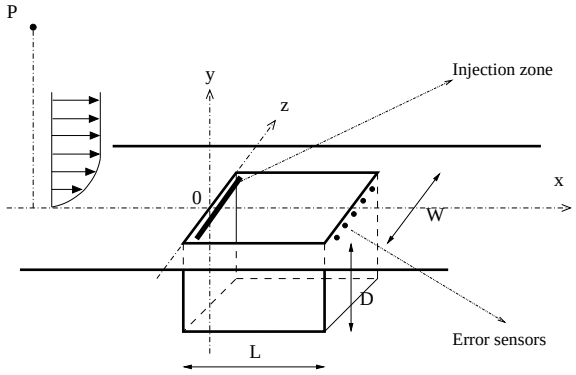

Figure 9: Simulated cavity layout.

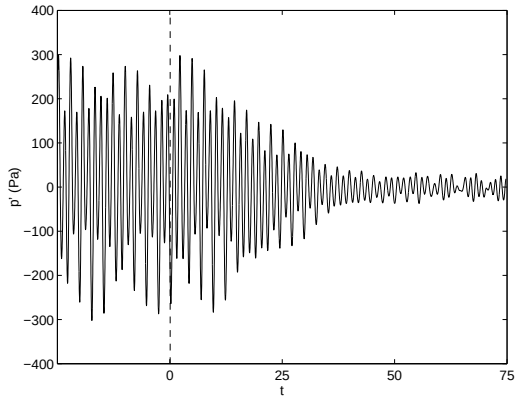

Figure 10: Numerical simulation of a closed-loop active control in a 3-D cavity. Time evolution of the pressure radiated at point P, see Fig. 9, before and after control. Control phase starts at $t = 0$. From Marsden *et al.* (2003).

more delicate aspects of the simulation. It was found that the total elimination of upstream instabilities, although possible for a short time, must be avoided in order to obtain a stable state. Indeed if the upstream instabilities become too small, they can very easily be perturbed and end up in phase with the injected control signal, leading to positive feedback and rapid divergence. The control algorithm should therefore not converge to an error value of zero, since this state is unstable. Rather than impose a non-zero sinusoidal error toward which to converge, a leaky-LMS approach with a strong leakage factor was used, to avoid the error signal becoming too small. This method both avoids having to establish *a priori* a target error signal to obtain, and also increases the algorithm's response speed to phase and frequency changes in the error signal. Fig. 10 displays the signal pressure measured at point P, and illustrates the noise reduction when the control system is started. Analysis of the flow, the sound field and details about implementation of the feedback loop are provided in Marsden *et al.* (2003).

7 Concluding remarks

Noise emission is of increasing importance, and some problems of current interest have been discussed in the light of the direct computation of aerodynamic noise. Some key points about the state of art are summarized to conclude this survey paper.

Numerics

Over the last years, significant progress have been done to improve accuracy of Navier-Stokes solvers, not only in terms of dissipation but also in terms of dispersion for time-dependent simulations. It must be observed that it is often easier to increase algorithm's accuracy than the number of grid points of the mesh. And this recommendation also holds for commercial codes. DNC has also contributed to emphasize the role of silent boundary conditions combining non-reflecting outflow boundary conditions and sponge layers.

Turbulence

Turbulence modelling in large-eddy simulations remains a open key-issue, at least for DNC, and needs to be objectively examinated with the knowledge of the transfer function of the numerical algorithm, as suggested by Domaradzki and Adams (2002) or more recently by Berland *et al.* (2008) for optimized finite-difference schemes. Simulation of realistic transitional shear layers at higher Reynolds numbers is still problematic and often leads to amplified local turbulence and noise sources. The methodology to specify the inflow boundary conditions of turbulent boundary layers in the framework of DNC likewise remains a challenging task, the reader may refer to Xu and Martin (2004) for a recent discussion. Finally, validation and analysis of unsteady results, convergence of statistics for signal processing or comparison with low-resolved PIV data require precaution. Moreover, two-point space-time correlations are of particular importance for noise generation.

Is there still a role for modelling ?

Aeroacoustics needs detailed understanding of noise generation mechanisms, not only to develop less expensive predictive models, but also to support the interpretation of experimental and numerical results. The identification of noise emissions, of couplings, of non-linear interactions or simulation of adaptive control loops including actuators need to be guided by theoretical approaches. Moreover, even from a more practical view, DNC cannot be the classical procedure for low Mach number flows often encountered in automotive applications. In this case, acoustic predictions will mainly be based on hybrid LES/CAA methods, such as Lighthill's theory (1952) or Ffowcs Williams & Hawkings (1969) wave extrapolation method.

As an illustration of this point, noise emitted by HVAC - heating, ventilating and air conditioning - is considered with the turbulent flow through a three-dimensional diaphragm used as a nominally test case. Snaphots of the Q-criterium and the mean axial velocity along the $x-y$ center plane are shown in Fig. 11. The mean flow is asymmetric behing the sudden expansion and is deviated, as expected by comparison with measurements, towards the upper side wall in the present case. Noise may then be computed in a second step by using a variational formulation of Lighthill's analogy in Fourier space proposed by Oberai *et al.* (2000) as implemented in some commercial codes. Such an approach requires the correct description of spatial source terms, typically of the form $\partial(\rho u_i u_j)/\partial x_j$ and a windowing of the source volume to control the truncation. These topics are well known in computational aeroacoustics. The application of a formulation based on space derivatives does not provide the best accuracy at a given mesh. Furthermore, for low Mach number flows, sources are compact and the characteristic scale of the source region and of the radiated acoustic field are therefore disparate. These remarks underline some difficulties for coupling a CFD code with a CAA code for noise predictions.

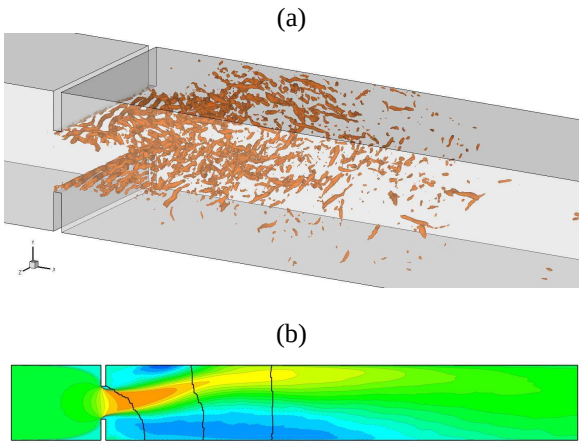

Figure 11: Turbulent flow inside a 3-D diaphragm: (a) snaphot of Q-criterium isosurfaces are plotted for the value $Q\times(h/u_\infty)^2 = 10$, and (b) averaged mean axial velocity along the $x-y$ center plane. The bulk velocity is $u_\infty = 20$ m.s^{-1} and the inlet channel height is $h = 0.035$ m yielding a Reynolds number $\mathrm{Re}_h = 4.7\times10^4$. The expansion ratio is $H/h \simeq 2.3$, the aspect ratio is $w/h \simeq 2.9$ and the length of the main channel is $L/h \simeq 14.3$. From Piellard *et al.* (2008).

Work in progress

Among different topics that can be mentioned, numerical study of more complex geometries involving high-Reynolds number flows requires the use of high-quality block structured grids. Several research teams develop such techniques with the aim of aeroacoustic simulations, as in Sherer and Scott (2005). Efforts are also now provided to develop unstructured approaches

for realistic applications, even if accuracy and robustness seem still difficult and costly to preserve. Accuracy is also difficult to retain for transonic and supersonic flows in the context of aeroacoustics applications.

Acknowledgments

The first author thanks the organizers of the 7th International ERCOFTAC Symposium on Engineering Turbulence Modelling and Measurements (ETMM7) for their invitation. The authors would like also to thank Julien Berland and Xavier Gloerfelt from SINUMEF, ENSAM Paris, Thomas Emmert and Philippe Lafon from Electricité de France & LaMSID, UMR CNRS 2832, and Mélanie Piellard from Delphi Thermal Systems, Luxembourg, for their contribution to this paper. The authors gratefully acknowledge the Institut du Développement et des Ressources en Informatique Scientifique (IDRIS) of the CNRS and the Centre de Calcul Recherche et Technologie of the CEA (the French Atomic Energy Agency) for providing CPU time on Nec computers and technical assistance.

References

Bailly, C. and Bogey, C. (2006), An overview of numerical methods for acoustic wave propagation, *European Conference of Computational Fluid Dynamics*, Eccomas CFD 2006, September 5-8, Egmond and Zee, The Netherlands, Paper 635, 1-16 (CD-ROM).

Berland, J., Bogey, C. and Bailly, C. (2006), Low-dissipation and low-dispersion fourth-order Runge-Kutta algorithm, *Computer & Fluids*, Vol. 35(10), pp. 1459-1463.

Berland, J., Bogey, C. and Bailly, C. (2007), Numerical study of screech generation in a planar supersonic jet, *Phys. Fluids*, Vol. 19, 075105, pp. 1-14.

Berland, J., Bogey, C. and Bailly, C. (2008), Investigation using statistical closure theory of the influence of the filter shape on scale separation in large-eddy-simulation, in revision for *Journal Of Turbulence, http://jot.iop.org/*.

Bogey, C. and Bailly, C. (2006a), Investigation of downstream and sideline subsonic jet noise using Large Eddy Simulations, *Theoretical and Computational Fluid Dynamics*, Vol. 20(1), pp. 23-40.

Bogey, C. and Bailly, C. (2006b), Large Eddy Simulations of transitional round jets: influence of the Reynolds number on flow development and energy dissipation, *Physics of Fluids*, Vol. 18, 065101, pp. 1-14.

Bogey, C. and Bailly, C. (2007), An analysis of the correlations between the turbulent flow and the sound pressure field of subsonic jets, *Journal of Fluid Mechanics*, Vol. 583, pp. 71-97.

Cattafesta III, L. N., Williams, D., Rowley, C. and Alvi, F. (2003), Review of active control of flow-induced cavity resonance, AIAA Paper 2003-3567, pp. 1-20.

Colonius, T. (2001), An overview of simulation, modeling and active control of flow/acoustic resonance in open cavities, AIAA Paper 2001-0076, pp. 1-12.

Colonius, T. (2004), Modeling artificial boundary conditions for compressible flows, *Annu. Rev. Fluid Mech.*, Vol. 36, pp. 315-345.

Colonius, T. and Lele, S. (2004), Computational aeroacoustics: progress on nonlinear problems on sound generation, *Progress in Aerospace Sciences*, Vol. 40, pp. 345-416.

Domaradzki, J. A. & Adams, N. A (2002), Direct modelling of subgrid scales of turbulence in large eddy simulations, *Journal Of Turbulence, http://jot.iop.org/.*, Vol. 3(024), pp. 1-19.

Emmert T., Lafon, P. and Bailly, C. (2007), Computation of Aeroacoustic Phenomena in Subsonic and Transonic Ducted Flows, *13th AIAA/CEAS Aeroacoustics Conference*, AIAA Paper 2007-3429, 1-26.

Ffowcs Williams, J. E. and Hawkings, D. L. (1969), Sound generation by turbulence and surfaces in arbitrary motion, *Phil. Trans. Roy. Soc. London*, Vol. 264, Ser. A, 1151, pp. 321-342.

Freund, J.B. (2001), Noise sources in a low-Reynolds-number turbulent jet at Mach 0.9, *J. Fluid Mech.*, Vol. 438, pp. 277-305.

Gloerfelt, X., Bogey, C. and Bailly, C., 2003, Numerical evidence of mode switching in the flow-induced oscillations by a cavity, *International Journal of Aeroacoustics*, Vol. 2(2), pp. 193-217.

Krothapalli, A., Hsia, Y., Baganoff, D. and Karamcheti, K. (1986) The role of screech tones in mixing of an underexpanded rectangular jet, *J. Sound Vib.*, Vol. 106(1), pp. 119-143.

Lighthill, M.J. (1952), On sound generated aerodynamically - I. General theory, *Proc. Roy. Soc. London*, Vol. 211, Ser. A, 1107, pp. 564-587.

Marsden, O., Gloerfelt, X. and Bailly, C. (2003) Direct noise computation of adaptive control applied to a cavity flow, *C. R. Mc., Acad. Sci. Paris*, Vol. 331(6), pp. 423-429.

Marsden, O., Bogey, C. and Bailly, C. (2008), Direct noise computation of the turbulent flow around a zero-incidence airfoil, to appear in *AIAA Journal*.

Meier, G.E.A., Grabitz, G., Jungowski, W.M., Witczak, K.J. and Anderson, J.S. (1978) Oscillations of the supersonic flow downstream of an abrupt increase in duct cross-section, *Mitteilung aus dem Max-Planck-Institut fuer Stroemungsforschung und der Aerodynamischen Versuchsanstalt*, Göttingen, Vol. 65.

Meier, G.E.A., Szumowski, A.P. and Selerowicz, W.C. (1990), Self-excited oscillations in internal transonic flows, *Prog. Aerospace Sci.*, Vol. 27, pp. 145-200.

Oberai, A. A., Ronaldki, F. and Hughes, T. J. R. (2000), Computational procedures for determining structural-acoustic response due to hydrodynamic source, *Comput. Methods Appl. Mech. Engrg.*, Vol. 190, pp. 345-361.

Piellard, M., and Bailly, C. (2008), Validation of a hybrid CAA method and application to the case of a diaphragm in a duct at low Mach number, *14th AIAA/CEAS Aeroacoustics Conference*, Paper 2008-2873.

Raman, G. (1999) Supersonic jet screech: half-century

from Powell to the present, *J. Sound Vib.*, Vol. 225(3), pp. 543-571.

Rowley, C.W. and Williams, D.R. (2006), Dynamics and control of high-Reynolds-number flow over open cavities, *Annu. Rev. Fluid Mech.*, Vol. 38, pp. 251-276.

Sherer, S. E. and Scott, J. N. (2005), High-order compact finite-difference methods on general overset grids, *J. Comput. Phys.*, Vol. 210, pp. 459-496.

Suzuki, T. and Lele, S. (2003) Shock leakage through an unsteady vortex-laden mixing layer: application to screech jet, *Journal Fluid Mech.*, Vol. 490, pp. 139-167.

Tam, C.K.W., Seiner, J.M. and Yu, J.C. (1986) Proposed relationship between broadband shock associated noise and screech tones, *J. Sound Vib.*, Vol. 110(2), pp. 309-321.

Tam, C.K.W. (1988) The shock-cell structures and screech tone frequencies of rectangular and non-axisymmetric supersonic jets, *J. Sound Vib.*, Vol. 121(1), pp. 135-147.

Tam, C.K.W. (1995) Supersonic jet noise, *Annu. Rev. Fluid Mech.*, Vol. 27, pp. 17-43.

Wang, M., Freund, J.B. and Lele, S.K. (2006), Computational prediction of flow-generated sound, *Annu. Rev. Fluid Mech.*, Vol. 38, pp. 483-512.

Xu, S. and Martin, M. P. (2004), Assessment of inflow boundary conditions for compressible turbulent boundary layers, *Phys. Fluids*, Vol. 16(7), pp. 2623-2639.